JOURNAL OF Applied Polymer SCIENCE

Preparation and Characterization of Hydrogel–Nanosilver Composites based on Copolymers from Sodium 2-Acrylamido-2-Methylpropanesulfonate

Hernán Valle,[1] Bernabé L. Rivas,[1] María R. Aguilar,[2] Julio San Román[2]

[1]Polymer Department, Faculty of Chemistry, University of Concepción, Casilla 160-C, 4089100 Concepción, Chile

[2]Biomaterials Department, Institute of Polymer Science and Technology, CSIC, Juan de la Cierva 3, 28006 Madrid, Spain

Correspondence to: B. L. Rivas (E-mail: brivas@udec.cl)

ABSTRACT: Hydrogel–nanosilver composites based on copolymers from sodium 2-acrylamido-2-methylpropanesulfonate (AMPS) were prepared. The silver nanoparticles (AgNPs, or nanosilver) were synthesized in aqueous media using citrate trisodium as stabilizing agent. The hydrogels were obtained by radical copolymerization of the monomers acrylamide (AAm)/AMPS and *N*-vinylpyrrolidone(VP)/AMPS in the molar ratio [1 : 1], using 3 and 6 mol % of *N*,*N*-methylene-bis-acrylamide (MBA) as a crosslinking reagent. The distribution of the monomers in both copolymers showed a tendency to moderately alternate because the product of their reactivity ratios was near to zero. The hydrogels were immersed in the colloidal dispersion of AgNPs, which generated hydrogen bonds between the carboxylic acid groups that cover the surface of the AgNPs and the pendant amide groups of the copolymers. The formation of the hydrogen bond was confirmed using solid-state ^{1}H NMR. The hydrogel–nanosilver composites with a lower percentage of MBA retained more silver. © 2012 Wiley Periodicals, Inc. J. Appl. Polym. Sci. 000: 000–000, 2012

KEYWORDS: composites; nanoparticles; nanowires and nanocrystals; copolymers

Received 5 August 2012; accepted 29 September 2012; published online
DOI: 10.1002/app.38655

INTRODUCTION

During the last 50 years, the increasing threat of resistance to antibiotics and the concern about the safety and the toxicity of topic antiseptics has resulted in a renewed interest in the ancient use of silver to treat bacterial infections in acute and chronic wounds.[1] It has been demonstrated that AgNPs <10 nm can cross the external membrane of bacteria and that once inside, they interact with the DNA, which prevents bacterial replication, and also interact with the sulfydryl groups of the enzymes involved in the oxidative phosphorylation, which produces bacterial death.[2] The effective concentration of AgNPs against bacteria is considerably lower compared to that of ionic silver (nanomolar levels vs. millimolar levels).[3] In addition, in comparison to bacterial cells, human cells are less sensitive to the toxic effect of AgNPs (and the silver ions), because human cells have a greater structural and functional complexity.[4]

AgNPs have a tendency to agglomerate in aqueous solutions and have difficulties in joining several surfaces.[5] To avoid these types of difficulties, several stabilizing agents are used; these agents interact with the nanoparticles (NPs) through adsorption processes. Currently, several polymeric stabilizing agents are used, but the most important are natural and synthetic polymers, dendrimers, latex particles, microgels, and hydrogels.[6] Three-dimensional polymeric networks of hydrogels impart excellent stability to AgNPs and reduce their toxicity by delaying their oxidation and release; therefore, during the last years, many researchers have shown an interest in developing new dressings to be used for wounds based on the hydrogel–AgNPs system.[7,8]

Similarly, the hydrogel–AgNPs dressings are considerably better that fabrics or films for treating skin burns because they have antibacterial activity and provide an efficient physical barrier against external bacteria, thereby maintaining a humid microenvironment around the wound surface, which is very helpful for the cicatrization process. Because the hydrophilic surface of the hydrogels in contact with biological fluids exhibits a very low interfacial free energy, proteins and cells do not tend to adhere to their surface. Because a hydrogel is a soft and gummy substance, it does not cause irritation to the surrounding tissues.[9]

Hydrogel–AgNPs composites with potential for application as dressings for deep and exudative wounds were obtained in this research. Hydrogels poly(*N*-vinylpyrrolidone-*co*-2-acrylamido-2-methylpropanesulfonate sodium) [poly(VP-*co*-AMPS)] and poly(acrylamide-*co*-2-acrylamido-2-methylpropanesulfonate

sodium) [poly(AAm-*co*-AMPS)] were selected for preparing the composites. The reactivity ratios of these copolymeric systems were determined by monitoring the reactions using the *in situ* ^{1}H NMR technique. The AgNPs obtained by the chemical reduction of aqueous silver nitrate ($AgNO_3$) and stabilized with sodium citrate were incorporated into the hydrogels by immersing the xerogel into the colloidal dispersion of AgNPs. The composites were characterized using solid state ^{1}H NMR, infrared spectroscopy, thermogravimetric analysis, scanning electron microscopy, and atomic absorption spectroscopy. It was demonstrated that the AgNPs are attached to the polymeric matrix of the composite through hydrogen bonds.

EXPERIMENTAL SECTION

Materials

AMPS was prepared by neutralizing 2-acrylamido-2-methylpropane sulfonic acid (>99%, Sigma–Aldrich) with 1*M* NaOH (Merck) in aqueous solution, and VP (99%, Sigma–Aldrich) was distilled under reduced pressure. The AAm (>98%) was provided by Fluka, and potassium persulfate (KPS, >99%), and MBA (>99%) were provided by Sigma–Aldrich. Formaldehyde (FA, 37%), trisodium citrate dihydrate (citrate, >99%) and $AgNO_3$ (>99%) were supplied by Merck. Ultrapure (UP) water obtained from a Milli-Q®water purification system was used in the experiments.

Synthesis and Characterization of the AgNPs

The chemical synthesis of the AgNPs was performed by intermittently heating an aqueous dissolution of 1 millimolar (m*M*) $AgNO_3$, 1 m*M* citrate, and 5 m*M* formaldehyde in a microwave oven. The number of heating cycles (ON: 20 s, OFF: 20 s) was 24 and then, the reactor temperature was immediately lowered using a cold water bath. The resulting colloidal dispersion of AgNPs was stored in the dark at 4°C in a glass container. The UV–visible absorption spectrum of the silver colloid in the range 200–800 nm was obtained using a Lambda 35 (Perkin Elmer) spectrophotometer, and UP water was used to adjust the baseline. The transmission electron microscopy images of the colloid were acquired with a JEOL JEM 1200 EXII (4-Å resolution) microscope equipped with an energy dispersive X-ray spectrometer (EDS). A drop of the colloid was placed onto a copper grid (150 mesh), coated with a thin film of carbon and dried at 35°C to obtain the images and their respective elemental analysis by EDS. Using the Zetasizer equipment (Malvern Instruments), electrophoretic mobility and dynamic light scattering (DLS) experiments were conducted to determine the zeta potential, mean size and size distribution of the AgNPs in the colloid.

Synthesis of Copolymers and Composites

Synthesis of Crosslinked Copolymers (Hydrogels). The copolymer systems, poly(VP-*co*-AMPS) and poly(AMPS-*co*-AAm) were synthesized in aqueous media with an equimolar composition of monomers in the feed, and their total concentration was 1*M* (15 wt %); 3–6 mol % of MBA as a crosslinking reagent and 1 mol % of KPS as an initiator were also used for each copolymer system (with respect to the total moles of monomer). The initiator was added after bubbling nitrogen gas into the monomer mixture for 10 min. The reaction was performed at 60°C for 24 h in a 40 mL Teflon tube. The reaction products were extracted from the tubes and soaked in UP water for 2 days to remove residual solute, and they were finally dried at 60°C in an air circulating oven.

Synthesis of Linear Copolymers. The same procedure used to synthesize the crosslinked copolymers was used to synthesize the linear copolymers, but the crosslinking reagent was not used and the total monomer concentration was reduced to 0.175*M* (2.5 wt %). The obtained linear copolymers were purified by dialysis (with a membrane of 3.5 kDa) and dried using a lyophilizer.

Preparation of the Composites. From each hydrogel synthesized according to the previous procedure (four hydrogels in total), two dried fractions of 3 g were collected. The first fraction was immersed in 500 mL of the silver colloid at 25°C, and it was removed from the colloid after 24 h and dried at 60°C in an air circulating oven. The first processed fraction (loaded with AgNPs) and the second intact fraction (free of AgNPs) were milled and sieved through a 100-μm sieve to obtain 1 g of dry powder per sample. All samples were stored in sealed vessels for further characterization.

Characterization of Copolymers and Composites

Spectroscopic Characterization. The crosslinked polymers (hydrogels) and their composites were analyzed using high-resolution magic angle spinning proton nuclear magnetic resonance (^{1}H HRMAS NMR) using a Bruker Avance 400 wide bore (89 mm) spectrometer operating at 9.4 T (proton Larmor frequency at 400.14 MHz). Twenty milligrams (20 mg) of each sample were impregnated with ~100 μL of deutered water and introduced into a zirconia rotor with a diameter of 4 mm. All of the spectra were acquired at room temperature using a crosspolarization/magic angle spinning (CP-MAS) probe for solid samples, a 90° pulse of 3.5 μs and a spinning rate of 5 kHz. The spectral width was 5 kHz, and 16 k data points and 16 scans were collected with a repetition rate of 5 s. The chemical shifts were referenced to internal deutered water, D_2O (4.86 ppm).

The linear copolymers were dissolved in D_2O at a concentration of 10 mg mL^{-1}, and the ^{1}H NMR spectra were acquired using a Mercury 400-BB spectrometer operating at a frequency of 400 MHz. The composition of each monomer in the copolymers was calculated based on the analysis of their spectra.

The each copolymerization of two copolymer systems studied (AAm: AMPS and VP: AMPS) was monitored using *in situ* ^{1}H NMR spectroscopy. To monitor the copolymerization, two reactions were prepared with different monomer compositions in the feed, and deutered water was used as the solvent. The compositions in the feed selected for the AAm: AMPS system were 30: 70 and 70: 30, and the ones selected for the VP: AMPS system were 30: 70 and 50: 50. The total monomer concentration was 0.175*M* (2.5 wt %), and KPS was used at a concentration of 1 mol %. Each reaction was performed in a resonance tube that was previously deoxygenated with nitrogen. A capillary tube filled with dichlorobenzene in deutered dimethylsulfoxide was placed inside of the resonance tube to serve as a reference signal.

Table I. Mean Diameters (ϕ) and Percentages of Different Particle Populations (%) from the Silver Colloid Prepared

		Population no. 1			Population no. 2			Total population			
Sample	Technique	Range (ϕ, nm)	Diameter (ϕ, nm)	%	Range (ϕ, nm)	Diameter (ϕ, nm)	%	ϕ<10 (%)	10<ϕ<25 (%)	ϕ>25 (%)	ϕ (nm)
Silver colloid	TEM	1.2-7.4	3.0 ± 1.0	58	8.7-82.7	35 ± 19	42	59	16	25	16 ± 20
	DLS	1.5-5.6	3.1 ± 0.4	-	14-164	50.7 ± 0.8	-	-	-	-	23.1 ± 0.3

The ^{1}H NMR spectra were acquired at 60°C using a Varian Inova 400 spectrometer programmed with the following parameters: pulse sequence of 7 μs, equivalent to a pulse of 90°; and acquisition of a spectrum (experimental point) every 120 s and spinning rate of 7 Hz. The spectra were normalized and integrated using the program MestReNova (version 6.0.2) to obtain the "instantaneous concentrations of monomers in feed," which were then processed using a mathematical model that allowed for the calculation of the reactivity ratios of the comonomers.[10]

The infrared spectra of the crosslinked copolymers and composites were obtained using a Spectrum One (Perkin–Elmer) spectrometer using the attenuated total reflection Fourier transform infrared spectroscopy (ATR–FTIR) method. The spectra were recorded with 32 scans and a resolution of 4 cm^{-1}.

Scanning Electron Microscopy (SEM) and Energy Dispersive X-ray Spectroscopy (EDS). The images of SEM of the dried composites were acquired with a microscope Hitachi Model SU-8000 operating at high vacuum. The EDS microanalysis was performed with a spectrometer QUANTAX 200 (Bruker) coupled to the scanning electron microscope.

Thermogravimetric Analysis (TGA). The thermogravimetric measurements were performed on a TA-Q500 thermobalance from TA Instruments. The experiments were carried out under a nitrogen flow of 50 mL min^{-1} and a heating rate of 10°C min^{-1} from 40 to 550°C.

Quantification of Total Silver Released from the Hydrogel-AgNPs Composites. Approximately 10 mg of each of the composites was independently immersed in 20 mL of UP water (sealed container) at 25°C with constant agitation. After 96 h, the insoluble material was separated from the aqueous medium by filtration with a nylon mesh of 80 μm (pore); the filtrates were subjected to acid digestion with 5 mL of concentrated nitric acid (65 wt %) and gentle heating to obtain a final volume of 10 mL. A series of standard solutions of ionic silver were also prepared using the same acid digestion conditions mentioned above. Finally, all of the samples were diluted with UP water until a final volume of 50 mL was obtained and analyzed by atomic absorption spectroscopy to determine the concentration of silver in each of the samples. In this experiment, a hollow silver cathode lamp and an air-acetylene flame with a wavelength of 328.1 nm were used.

RESULTS AND DISCUSSION

Silver Nanoparticles

The UV-visible absorption spectrum of the obtained colloid exhibited a pronounced peak at 434 nm that corresponds to the surface plasmon resonance (SPR) band of the AgNPs.[11] The surface plasmon resonance phenomenon is defined as the oscillation of the charge density that can exist in an interface metal-dielectric.[12] The zeta potential value was −47.2 ± 1.3 mV, which indicates a high stability of the nanoparticles and a tendency to maintain their initial nanosize without forming aggregates.[13] The negative electric charge close to the surface of the AgNPs is generated by citrate ions that surround the particle surface and that function as stabilizer agents.[14] Based on the pH value of 6.5 obtained from the colloid and the acid dissociation constants of citric acid ($pK_{a1} = 3.13$, $pK_{a2} = 4.76$, $pK_{a3} = 6.40$) reported in literature, the coexistence of 44% of divalent citrate species and 56% of the trivalent ones can be inferred.[15]

The DLS experiment conducted on the colloid produced a particle size distribution expressed as a function of the intensity of the dispersed laser light. The distribution of sizes was bimodal with a meaningful amplitude, which is consistent with the recorded polydispersity index of 0.596.[16] This bimodal distribution suggests the existence of two populations of particles with very different sizes in the colloid. Some researchers recommend reporting the complete bimodal distribution, specifying the mean diameter of each population and the total mean diameter with relevant standard deviations, regardless of whether the standard deviation may be higher than the mean in some cases; this recommendation is based on a biological perspective because omitting any fraction of particles in trials such as those related to toxicity can be a negative factor for achieving a proper interpretation of the data.[16] For this reason, Table I shows prior statistical parameters of both populations and those of total particles constituting the obtained colloid.

The analysis of the colloid with the DLS technique revealed a mean particle diameter of population No. 1 that was ~16 times less than that of population No. 2 (see Table I). Both populations of AgNPs were also observed using the TEM technique; additionally, it was established that the majority of the NPs exhibit a spherical form (see Figure 1). Note that although both techniques coincide with the bimodal distribution, the DLS technique has a particle size discrimination power of 1 : 3 in multimodal samples[17]; therefore, the values of the average diameter of each population obtained using the DLS technique showed a variation with respect to the ones obtained with the TEM technique. The low size discrimination power of the DLS

Applied Polymer SCIENCE

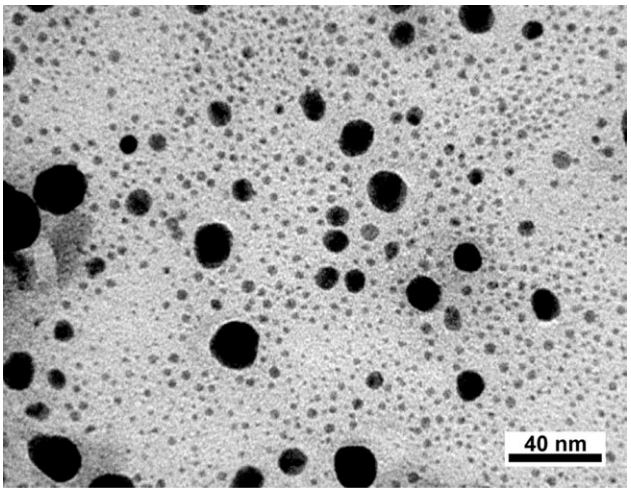

Figure 1. TEM image of the AgNPs in the colloid obtained. The dimension of the scale bar is 40 nm.

technique is due to the fact that the intensity of light dispersed by a particle is proportional to the power of six of its diameter. This fact may explain the similar results obtained using the DLS and TEM techniques for the mean diameter of population No. 1 (small particles) and the different results obtained using the same techniques for the mean diameter of population No 2 (large particles) (see Table I). Additionally, during the DLS analysis of a bimodal sample, similar to the one obtained, it is necessary to consider that the intensity of the dispersed light (% intensity) does not represent the "number of NPs" with the indicated diameter because a small number of large particles can result in a higher intensity signal than the signal generated by a high number of small particles[18]; this difficulty can be overcome with the direct observation of the NPs using the TEM technique because this method allows for the particles to be counted and the diameters to be measured without ambiguity. Although these differences exist between the techniques, it can still be observed that the mean diameter of particles of population N°1 is lower than that of population N°2. The presence of the two populations of NPs in the colloid is due to the fact that before being reduced by the formaldehyde, the silver cations are grouped as two different chemical species in the initial reaction solution, which is due to their equimolar relationship with citrate anions and low concentrations of reagents; the first and most abundant species is the "colloidal silver citrate," whereas the second one is known as "silver complexes," where silver ions are coordinated with citrate anions; "colloidal silver citrate" promotes the formation of AgNPs with a LOW mean diameter and a NARROW size distribution, whereas "silver complexes" promote the formation of NPs with a HIGH mean diameter and a WIDE size distribution through their reduction with formaldehyde.[19]

Note that over 50% of the total NPs present in the colloid exhibited diameters that are <10 nm (see Table I, TEM results); therefore, they are in compliance with size requirements to exhibit antibacterial activity, according to Morones et al.[2]

Hydrogels and Linear Copolymers

The obtained hydrogels were soft and brittle solids with a transparent appearance and adopted the form of the reaction vessel (cylindrical); they swelled and fragmented after being cut into disc shapes (with a thickness of 5 mm) and dipped in UP water, to remove residues from the reaction. After drying in an oven, all of the hydrogels were significantly reduced in size and became a compact, hard and white solid. The reaction yields for the four synthesized hydrogels (crosslinked copolymers) and the numbers assigned to each one to facilitate their identification are summarized in Table II.

Table II. Reaction Yields (%) Obtained from the Hydrogels Synthesis

Hydrogel number	Feed composition	Yield (%)
7	VP:AMPS[1 : 1]—3 mol % MBA	45
11	VP:AMPS[1 : 1]—6 mol % MBA	68
15	AAm:AMPS[1 : 1]—3 mol % MBA	97
22	AAm:AMPS[1 : 1]—6 mol % MBA	98

The ^{1}H HRMAS NMR spectrum of hydrogel 15 is shown in Figure 2. Three signal regions can be observed, which confirm the polymerization of the monomers AAm, AMPS, and MBA. This spectrum also confirmed the absence of residual monomers because the vinyl signals did not appear between 5.5 and 6.5 ppm.[20] The region 1 is located in the high field of the NMR spectrum between 1.0 and 3.0 ppm, and it is generated by all of the protons of the polymer backbone (signals A1, A2, B1, B2, M1 and M2) and the geminal methyl groups of the AMPS monomer residue (A3, A4). The region 2, located between 3.0 and 4.2 ppm, is solely due to the methylene group next to the sulfonate group of the polymerized AMPS (signal A5). Finally, the region 3 is located at the low field of the spectrum between 7.0 and 8.0 ppm, and it is generated by the amide groups of the polymerized AAm and AMPS monomers (A6, B3, M4).[21]

Figure 3 shows the ^{1}H HRMAS NMR spectrum of hydrogel 7. The signal at 5.93 ppm probably could have been generated by: (i) one of the two groups of the MBA vinyl protons, which did not react during polymerization and remained as a pendant group of the copolymer[22] and/or (ii) all vinyl protons of residual MBA molecules which did not react during polymerization and remained trapped in the polymer matrix as free monomer.

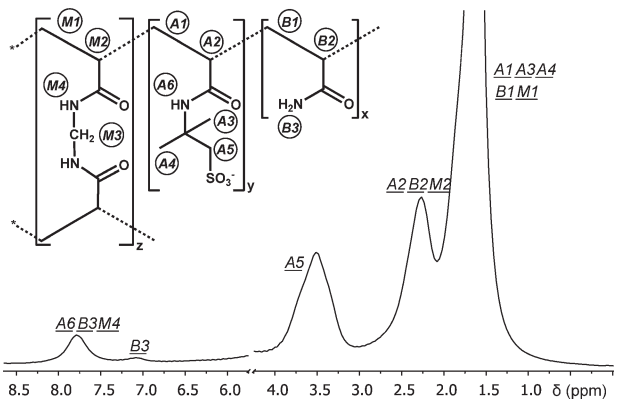

Figure 2. ^{1}H HRMAS NMR spectrum of the hydrogel 15.

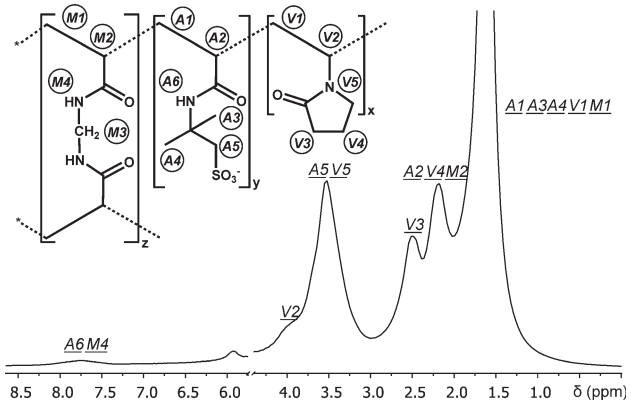

Figure 3. ^{1}H HRMAS NMR spectrum of the hydrogel 7.

The above suggests that a more exhaustive aqueous extraction of residual solute from the hydrogel 7 must be performed. There were no other vinyl signals between 5.5 and 6.5 ppm, which confirms the absence of other residual monomers. Three signals regions with the same ranges of chemical shift (ppm) as the previous case can be observed, and were also numbered in the same way (Region 1, 2, and 3). The Region 1 has a diverse origin that includes the protons of the polymer backbone (signals A1, A2, V1, M1 and M2) with the exception of those belonging to the CH groups attached to the pyrrolidone ring (signal V2), the methylene groups that are more protected inside the pyrrolidone ring (signals V3, V4) and the geminal methyl groups of the AMPS monomer residue (signals A3, A4). The Region 2 is generated by the CH_2 and CH groups that are attached to the nitrogen of the pyrrolidone ring (V5, V2) and by the methylene group next to the sulfonate of the polymerized AMPS (A5). Finally, the Region 3 is generated by the amidic proton signal belonging to the polymerized AMPS and MBA (A6, M4).[23,24,21]

The methylene protons designated as "M3" in the Figures 2 and 3, which are located in the —$CONHCH_2NHCO$— units of the polymerized MBA, could not be assigned to its respective signal in the spectrum (at 4.6 ppm) since it is overlapped by broad and intense signal of the solvent (D_2O/H_2O, 4.4–5.4 ppm). Additionally the solvent signal has been deleted for clarity.

Note that determining the exact composition of the three monomers in the obtained crosslinked copolymers is impossible because only two regions of measurable signals are present and the calculations require a minimum of three regions (one per monomer). The Region 3 cannot be used in the calculations because these signals result from amidic hydrogen that are partially exchanged with deuterium from the deuterated water[25]; therefore, the integrated areas of these signals indicate that there are fewer hydrogen atoms than those actually present in the polymer.

With the intention of obtaining the approximate composition of each monomer in the crosslinked copolymers, their respective linear copolymers without crosslinking (MBA) were synthesized and then analyzed using solution ^{1}H NMR.

The obtained linear copolymers, poly(VP-*co*-AMPS)[1 : 1] and poly(AAm-*co*-AMPS)[1 : 1], were white solids that appeared as finely divided flakes, which were highly soluble in water, and their reaction yields were 52 and 74%, respectively. The ^{1}H NMR spectra of the linear copolymers in deuterated water were very similar to the solid-state ^{1}H HRMAS NMR spectra of their corresponding crosslinked structures (hydrogels), both in terms of the signals and in their chemical shifts; therefore, the identification of the linear copolymers signals was performed the same way as that used for the hydrogels (see Figures 2 and 3). Although the hydrogels and linear polymers only differ by the absence of MBA in the linear polymers, the similarity of their NMR spectra is due to the following: (i) the overlapping signals that occur between the MBA and other polymerized comonomers, and (ii) the low concentration of MBA with respect to the other monomers in the hydrogels.

Note that the spectra of the linear copolymers exhibited an improvement in spectral resolution and that amidic protons were not detected, unlike what was observed in the spectra of the respective hydrogels. The absence of the amidic proton signals in the spectra of both systems is due to the complete exchange of protons of the amidic groups with deuterated water.

Similar to their crosslinked versions, linear copolymers also showed the same signals regions (Region 1, 2 and 3). Based on the assignments of the proton groups of Regions 1 and 2 to the molecular structure of each copolymer (see Tables III and IV), equations were formulated to calculate the respective monomer compositions as a function of the area of the signals of the regions mentioned. The areas of Regions 1 and 2 were normalized and integrated using the program MestReNova (Version 6.0.2). The values of the integrals were replaced in the respective composition equations, and the calculations produced the monomer molar fractions (cumulative) in each copolymer.

The composition equations formulated from the poly(VP-*co*-AMPS) spectrum are:

Table III. The ^{1}H NMR Spectrum Signals Identification of Poly(AAm-*co*-AMPS)

Regions of the spectrum poly(AAm-*co*-AMPS)	Signals	Comming from	Type of proton	Number of protons
Region 1 (1–3 ppm)	A1, A2	AMPS	CH_2 and CH of the main chain	3
	A3, A4	AMPS	CH_3 geminals	6
	B1, B2	AAm	CH_2 and CH of the main chain	3
Region 2 (3–4.2 ppm)	A5	AMPS	CH_2 neighbour to sulfonate group	2

Table IV. The ^{1}H NMR Spectrum Signals Identification of Poly(VP-*co*-AMPS)

Regions of the spectrum poly(VP-*co*-AMPS)	Signals	Comming from	Type of proton	Number of protons
Region 1 (1–3 ppm)	A1, A2	AMPS	CH_2 and CH of the main chain	3
	A3, A4	AMPS	CH_3 geminals	6
	V1	VP	CH_2 of the main chain	2
	V3, V4	VP	CH_2 more protected to the ring	4
Region 2 (3–4.2 ppm)	A5	AMPS	CH_2 neighbor to sulfonate group	2
	V2, V5	VP	CH and CH_2 neighboring to the ring	3

$$[VP] = \frac{V}{A+B} \quad (1)$$

$$[AMPS] = \frac{A}{A+V} \quad (2)$$

$$V = \frac{(I_{A1.A2.A3.A4.V1.V3.V4}) - 9A}{6} \quad (3)$$

$$A = \frac{(I_{A5.V2.V5}) - 3V}{2} \quad (4)$$

where [VP] and [AMPS] are the molar fractions of VP and AMPS in the copolymer, respectively. "V" is the value of the integral of a proton originated for all of the VP residues in the copolymer; and "A" is the value of the integral of a proton originated for all of the AMPS residues in the copolymer. "$I_{A5.V2.V5}$" is the value of the integral of Region 2, and "$I_{A1.A2.A3.A4.V1.V3.V4}$" is the value of the integral of Region 1. For the case of poly (AAm-*co*-AMPS), the following equations were obtained:

$$[AAm] = \frac{B}{A+B} \quad (5)$$

$$[AMPS] = \frac{A}{A+B} \quad (6)$$

$$B = \frac{(I_{A1.A2.A3.A4.B1.B2}) - 9A}{3} \quad (7)$$

$$A = \frac{I_{A5}}{2} \quad (8)$$

where [AAm] and [AMPS] are the molar fractions of AAm and AMPS in the copolymer, respectively. "B" is the value of the integral of a proton originated for all of the VP residues in the copolymer; "A" is the value of the integral of a proton originated for all of the AMPS residues in the copolymer. "I_{A5}" is the value of the integral of Region 2 and "$I_{A1.A2.A3.A4.B1.B2}$" is the value of the integral of Region 1.

The results of the composition calculations for the poly(VP-*co*-AMPS) produced the following monomer mole fractions: 0.42 for VP and 0.58 for AMPS. In the case of poly(AAm-*co*-AMPS), the mole fractions of AAm and AMPS were 0.55 and 0.45, respectively.

Reactivity of the Comonomers

As mentioned in the "Experimental section", the copolymerization reaction was monitored using *in situ*^{1} H NMR to quantify the concentrations of the monomers at different times to obtain the reactivity ratios of the comonomers. Initially, a total concentration of monomers of 15 wt % in the feed was examined (which corresponds to the concentration of our crosslinked or hydrogel systems), but the comonomers could not be quantified because the reaction mixture quickly increased its viscosity (possibly due to the gel effect); this impeded its analysis using the ^{1}H NMR technique, which requires complete solubility of the sample. To overcome this drawback, the copolymerization reactions were prepared with monomers in the feed at a concentration of 2.5 wt %, which ensured the solubility of the reaction mixtures in each copolymer system under study. As an example, Figures 4 and 5 present the spectra of the AAm: AMPS [30 : 70] and VP : AMPS [30 : 70] systems at different reaction times and the protons used for the determination of the monomer concentrations. The dichlorobenzene signal could also be observed, which was used as a reference for the quantitative analysis (at ~8.1 ppm).

The monomer concentrations obtained at different times ($[M_1]$ and $[M_2]$) were submitted to a "nonlinear least squares fit" using the "terminal model copolymerization equation" in its integrated form [eq. (9)], which is shown below:

$$y = y_0 \left(\frac{x}{x_0}\right)^{\frac{b}{1-b}} \cdot \left[\frac{1-b+(a-1)x}{1-b+(a-1)x_0}\right]^{\frac{ab-1}{(1-a)(1-b)}} \quad (9)$$

where "x" = $[M_1]/[M_2]$ = [VP]/[AMPS] or [AAm]/[AMPS]; "y" = $[M_2]$ = [AMPS]; "a" = r_1 (r_{VP} or r_{AAm}); and "b" = r_2 (r_{AMPS}).

The use of eq. (9) with different $x_0 - y_0$ values in the same reaction, that is, to different experimental points $x_t - y_t$ that are assumed to be initial points of the reaction system under study, produced different values of r_1 and r_2 for each fit.

In both copolymer systems, [poly(VP-*co*-AMPS) and poly (AAm-*co*-AMPS)], the pairs of $r_1 - r_2$ values obtained for each of the reactions with different monomer compositions in the feed (two for each copolymer system) exhibited a linear tendency when they were plotted, and the intersection point of the obtained lines (see Figure 6) corresponds to the optimum value of the reactivity ratios.[10]

The intersection of the two lines in Figure 6(a) generated values of $r_{VP} = 0.15$ and $r_{AMPS} = 0.22$ for the poly(VP-*co*-AMPS) system. The reactivity ratios of this system were previously studied by Kurenkov and Zhelonkina[26] but with a 10% w/v of monomers in the feed, and the reported values were $r_{VP} = 0.15$ and $r_{AMPS} = 0.35$.

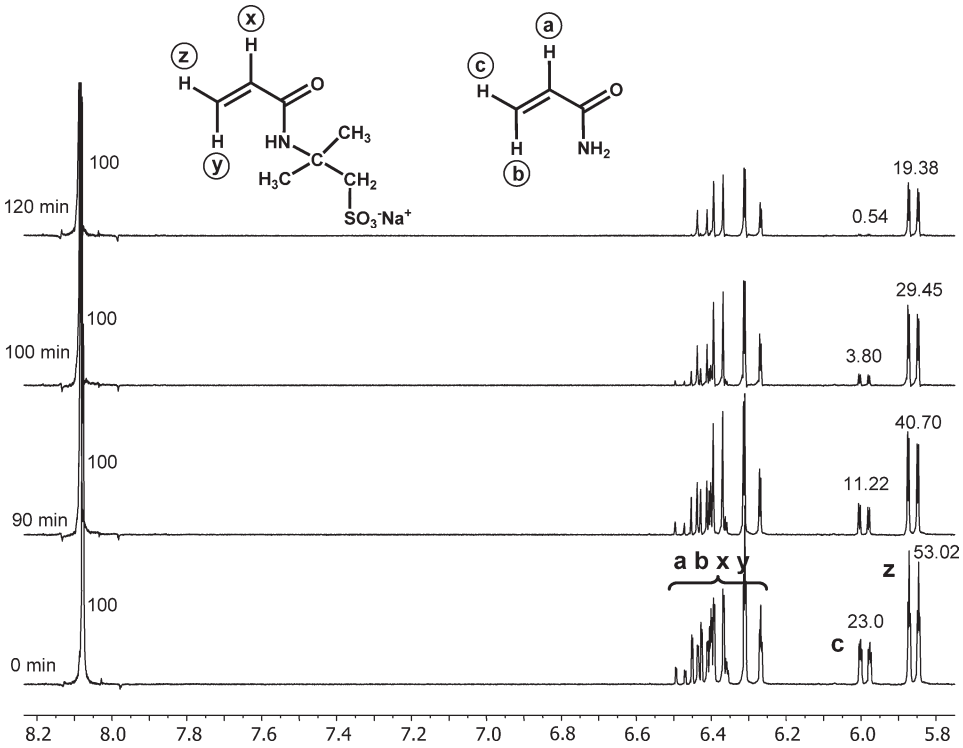

Figure 4. Vinylic region of some representative ^{1}H NMR spectra of the copolymerization reaction at different times of the AAm: AMPS (30: 70) system.

In the case of the poly(AAm-*co*-AMPS) system, the intersection point of the two lines in Figure 6(b) corresponds to the values of $r_{AAm} = 1.1$ and $r_{AMPS} = 0.16$. In previous experiments, Travas–Sejdic and Easteal[27] observed values of $r_{AAm} = 1.05$ and $r_{AMPS} = 0.42$, but the total monomer concentration used in the feed was 0.85*M*, which is approximately five times greater than that used in our experiment (0.175*M* = 2.5 wt %).

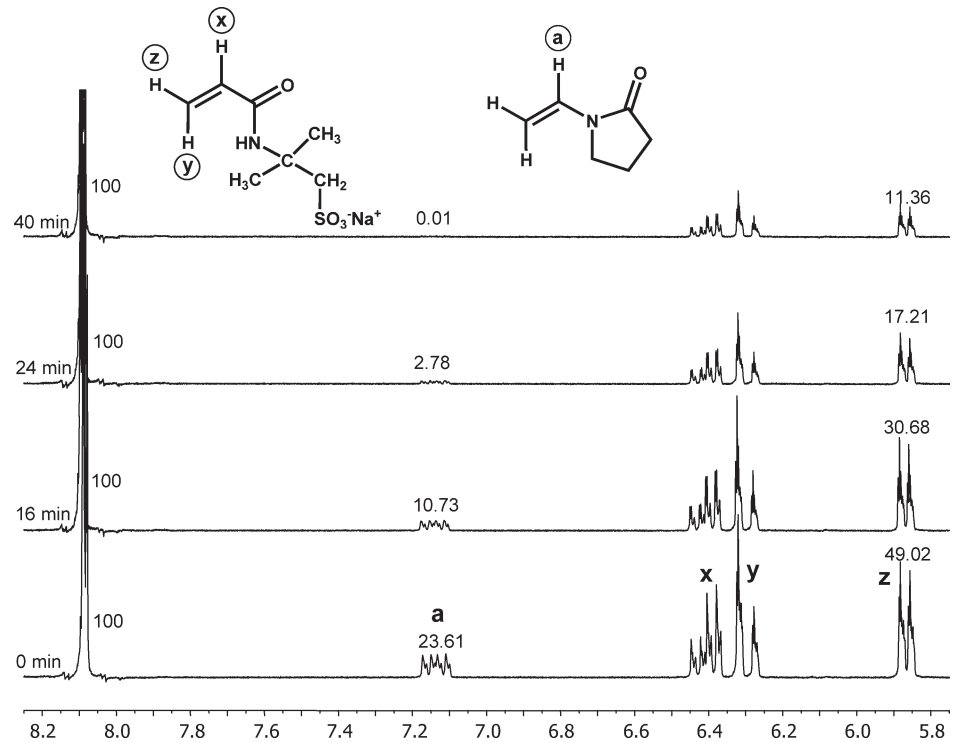

Figure 5. Vinylic region of some representative ^{1}H NMR spectra of the copolymerization reaction at different times of the VP: AMPS (30 : 70) system.

Applied Polymer SCIENCE

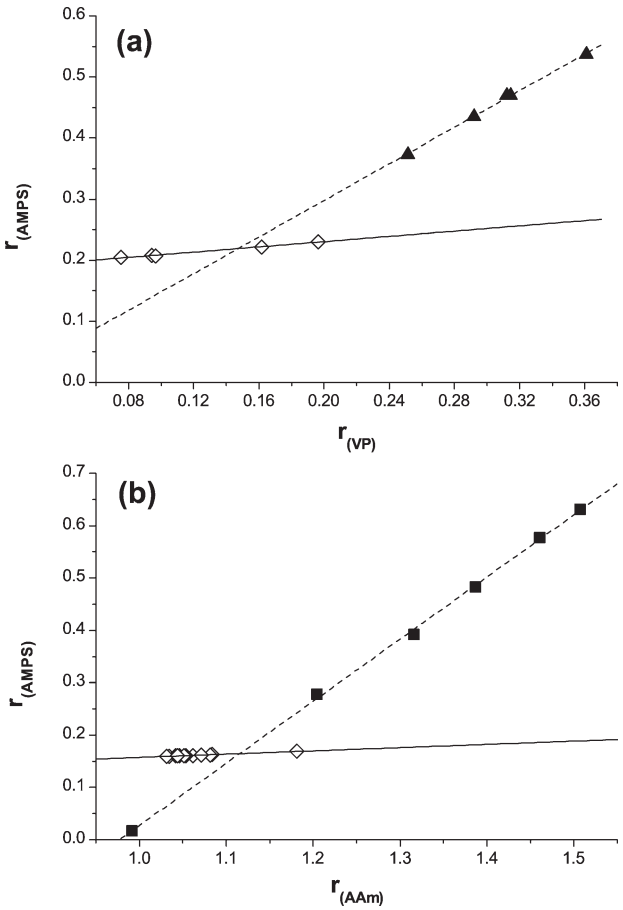

Figure 6. Diagrams of reactivity ratios of the systems: (a) VP : AMPS and (b) AAm: AMPS. Empty diamonds: reaction with monomers feed composition of 30 : 70, solid triangles: reaction with monomers feed composition of 50 : 50, and solid squares: reaction with monomers feed composition of 70 : 30.

In both cases, the obtained values of r_{AMPS} (r_2) were lower than those reported for the same systems with higher total concentrations of monomers. This result can be explained by the decrease in the ionic strength of the medium when the total concentration of monomers is reduced; at lower ionic strengths, there is a lower shielding of charges (higher Debye–Hückel length) between the anionic monomer ($AMPS^-$) and the partly anionic growing chain, and hence, the electrostatic repulsion increases, which leads to the increasing rate constant of heteropropagation (k_{21}) with respect to that of homopropagation (k_{22}), and thus, the value of $r_2 = k_{22}/k_{21}$ decreases.[28]

The executable computer program "Conversion.exe" developed by Gallardo et al.[29] (which is based on the terminal model of copolymerization) was applied to the values of the obtained reactivity ratios; the data set generated by the Conversion.exe program was read and plotted by the Surfer graphing software (version 10.7.972) to obtain 3D graphics that predict the evolution of the instantaneous copolymer molar fraction (F_{M1}) as a function of the conversion and the initial molar fraction in the feed (f_{M1}) (see Figures 7 and 8).

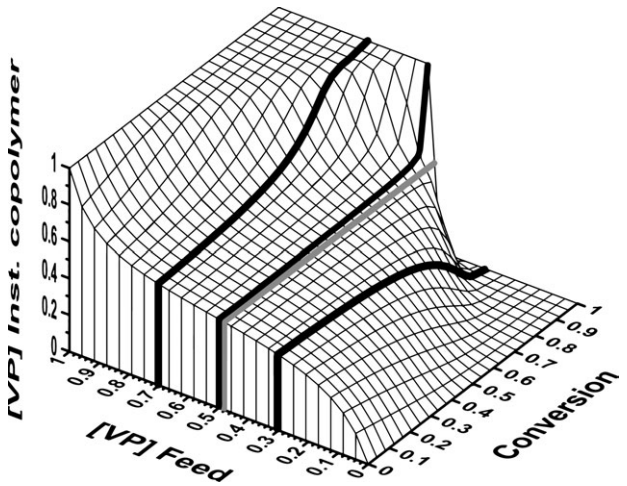

Figure 7. VP instantaneous copolymer molar fraction for the system poly(VP-*co*-AMPS) as a function of conversion and VP feed molar fraction. The black lines represent the course of the reactions for a specific VP feed molar fraction (f_{VP} = 0.3, 0.5, 0.7) and the gray line represent the course of the reaction for the azeotropic point (AZP = f_{VP} = 0.478).

The monomers of the poly(VP-*co*-AMPS) system exhibited reactivity ratios less than unity (r_{VP} = 0.15 and r_{AMPS} = 0.22), which is characteristic of an azeotropic copolymerization. In this type of copolymerization, there is a unique feed monomer composition (f_{VP}) that produces the same copolymer monomer composition (F_{VP}) at any conversion (azeotropic point: AZP); in our case, this value is $f_{VP} = F_{VP}$ = 0.478 (see gray line in Figure 7). Another important feature of the system is the moderate tendency to generate an alternating structure because both monomers and propagating species preferentially react with the opposite monomer.[30] Additionally, the VP feed molar fractions that lie higher and lower than the azeotropic point (see black lines in Figure 7) respectively produce the same VP instantaneous copolymer molar fractions,

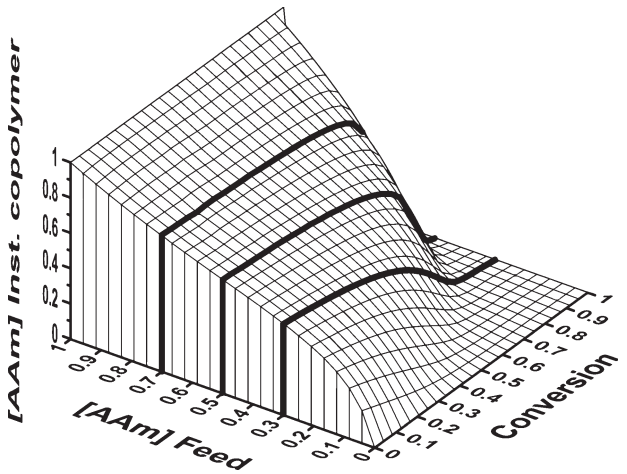

Figure 8. AAm instantaneous copolymer molar fraction for the system poly(AAm-*co*-AMPS) as a function of conversion and AAm feed molar fraction. The black lines represent the course of the reactions for a specific AAm feed molar fraction (f_{AAm} = 0.3, 0.5, 0.7).

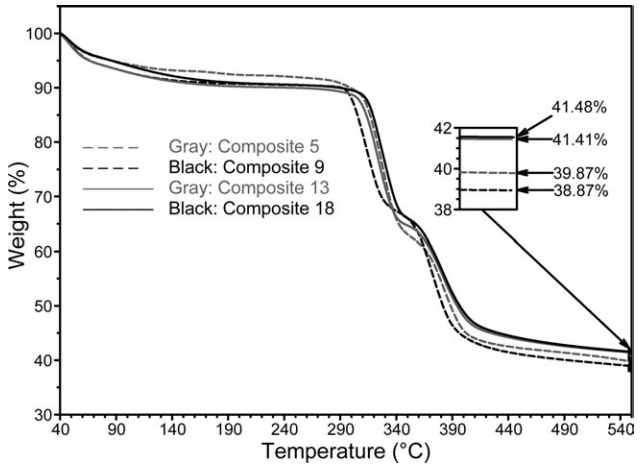

Figure 9. Effect of monomeric composition and the crosslinker amount in the thermogravimetric behavior of the composites prepared with the silver colloid (samples: 5, 9, 13, and 18).

but only until intermediate conversions (0.5 approximately), because from that point on, the VP feed molar fractions that lie higher than the AZP increase and those that lie lower than the AZP decrease. This result implies that the end sequences are rich in VP for the first case, whereas for the second case, the end sequences are rich in AMPS. The type of copolymerization followed for the poly(AAm-*co*-AMPS) system also qualifies as "moderately alternating" because the product of the reactivity ratios is close to zero ($r_{AAm} \times r_{AMPS} = 0.18$); but there is no azeotropic point (AZP), as in the case of the poly(VP-*co*-AMPS) system, because $r_{AAm} \geq 1$ (1.1) and $r_{AMPS} \leq 1$ (0.16).[30] The reactions with different AAm feed molar fractions produce the same AAm instantaneous copolymer molar fractions but only until 30% of conversion because at higher conversions, the fractions begin to gradually decrease. This behavior implies that the end sequences are rich in the less reactive monomer, AMPS (see Figure 8).

Table V. Volumes of Retained Colloid per Gram of Dried Hydrogel and Percentages (wt %) of Total Silver Released from the Composites after Being Immersing them in milli-Q Water During 96 h

Composite (no.)	Hydrogel (hydrogel no.)	mL of colloid per g of dry hydrogel	Ag (%) released in water
5	VP:AMPS[1 : 1]—3 mol % MBA (7)	115	2.42
9	VP:AMPS[1 : 1]—6 mol % MBA (11)	40	0.34
13	AAm:AMPS[1 : 1]—3 mol % MBA (15)	40	0.67
18	AAm:AMPS[1 : 1]—6 mol % MBA (22)	20	0.56

Hidrogel-AgNPs Composites

The dried composites exhibited a darker color than their origin hydrogels, which were not immersed in silver colloids. The obtained thermograms of the composites are shown in Figure 9. Based on the thermograms can be concluded that the VP : AMPS system (composites 5 and 9) increases its residual weight percentage as it decreases its crosslinker percentage. When the crosslinker reagent percentage decreases, the hydrogels improve their ability to swell and, as a consequence, experience an increase in the silver colloid volume retained in their interior, which implies a larger amount of loaded nanoparticles.[8,31] In the case of the AAm: AMPS system (composites 13 and 18), the variation of the content of the crosslinking agent has very little effect on the residual weight percentages. The thermogram data are in good agreement with the percentages (wt %) of total silver released by the composites in water (see Table V). From the results recorded in Table V note that among the four composites prepared, the composite No. 5 releases higher silver amount, therefore it could be much more effective against bacteria than others ones and

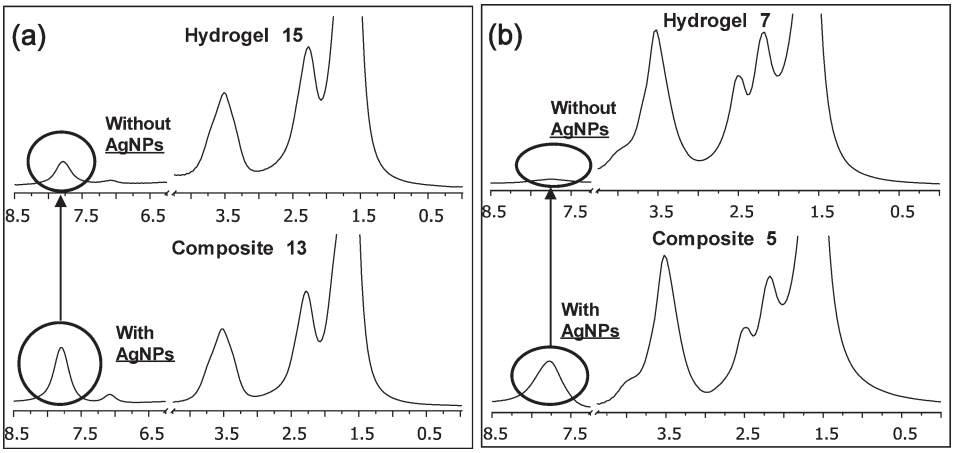

Figure 10. Comparison of ^{1}H HRMAS NMR spectra between: (a) composite 13 and hydrogel 15, (b) composite 5 and hydrogel 7. The signal intensity of the amidic protons (shown in the circles) is higher in composites.

Applied Polymer SCIENCE

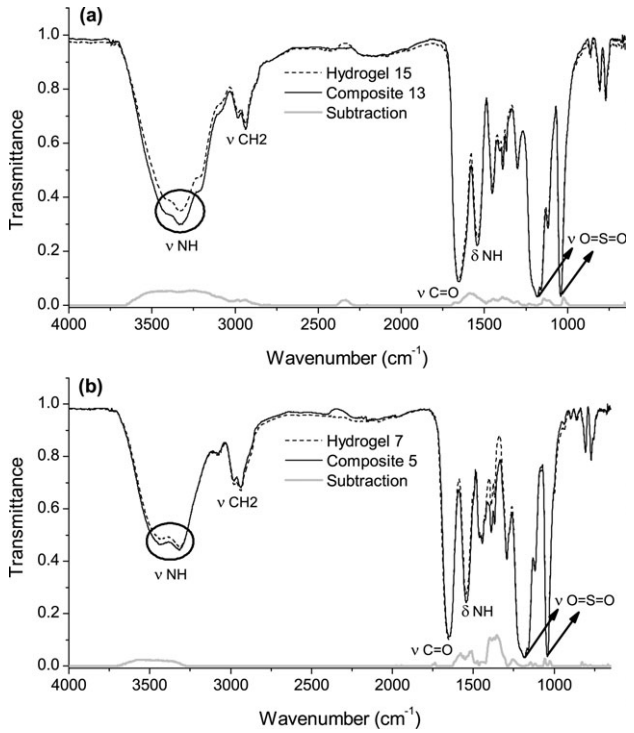

Figure 11. Comparison of ATR-FTIR spectra between: (a) composite 13 and hydrogel 15, (b) composite 5 and hydrogel 7. The amino groups stretching frequencies (shown in the circles) are more intense in the spectra of the composites.

hence, could be considered as potential candidate for exudative wounds treatment.

The ^{1}H HRMAS NMR spectrum of composite 13 was very similar to that obtained from hydrogel 15, with the difference that the former exhibited a higher intensity in the amidic protons signal [see Figure 10(a)]. The same result was obtained when the spectrum of composite 18 was compared with that of the hydrogel 22; the only difference between the above-mentioned first pair of materials and the second one, is the amount of MBA used during its synthesis (3 mol % vs. 6 mol %).

As in the previous cases, when the solid-state ^{1}H NMR spectrum of the composite 5 was compared with that of the hydrogel 7, the only difference observed was the higher signal intensity of the amide proton in the composite [see Figure 10(b)]; although the monomer composition and the concentration of MBA (3 mol %) are equal for both, the AgNPs incorporated into the composite cause the observed spectral difference. A result very similar to the one detailed above was obtained when the spectra of the composite 9 and the hydrogel 11 (containing 6 mol % MBA) were compared.

A possible explanation for the observed differences between hydrogels loaded with silver nanoparticles and those that were not loaded is the following: the surfaces of the AgNPs are surrounded with citrate molecules that can form hydrogen bonds with the amide pendant groups of the main chain of the copolymer.[32] With the formation of these hydrogen bonds, is substantially reduced the proton exchange between the amino groups and the deuterated water, and therefore, considerably more protons are detected in the NMR experiment.[25]

Table VI. The ATR-FTIR Spectrum Peaks Identification of the Hydrogels Poly(VP-*co*-AMPS) and Poly(AAm-*co*-AMPS)

Peak (cm^{-1})	Attributed to
3439–3220	stretching (ν) N—H of amine groups
2980–2936	stretching (ν) CH_2 symmetric and unsymmetric
1655–1650	stretching (ν) C=O of amides
1544–1543	bending (δ) N—H of amine groups
1183–1182	stretching (ν) O=S=O asymmetrics
1040	stretching (ν) O=S=O symmetrics

A comparative analysis of the ATR-FTIR spectra between some composites and their respective original hydrogels is shown in Figure 11 as an example; differences in the signal intensity corresponding to the amino groups stretching frequencies were observed (between 3439 and 3220 cm^{-1}). These signals were more intense for the composites,[31] which confirms the results obtained by solid-state ^{1}H NMR. The IR spectra of all samples indicated the presence of characteristic functional groups of the expected copolymers (see Table VI) and the absence of vinyl signals (*ν*C=C to 1635–1620 cm^{-1}).[33] This result is evidence of

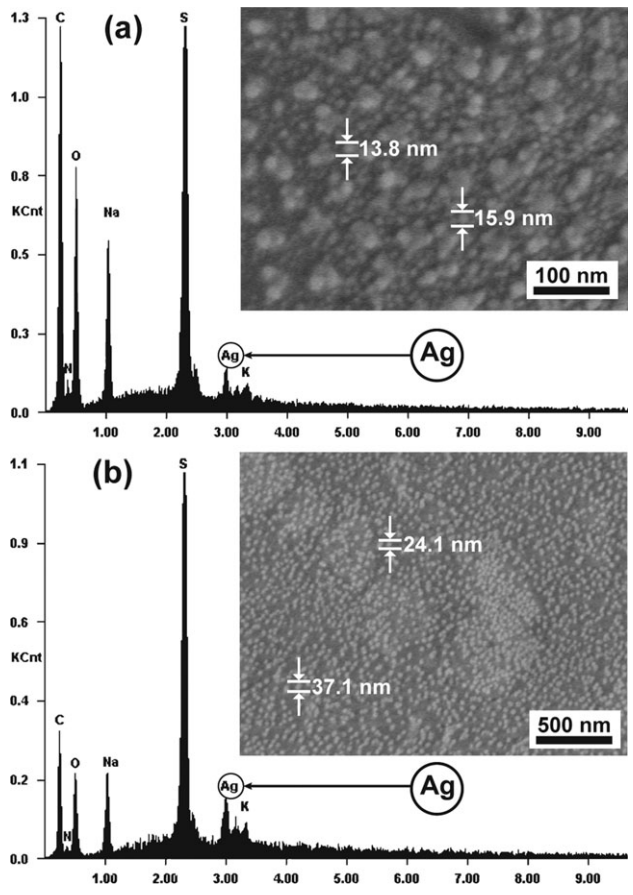

Figure 12. Scanning electron micrograph of outer surface (inset) and cross-section EDS spectrum of: (a) composite 5, (b) composite 13.

the copolymerization of the monomers and the purity of the obtained product. Similar results were obtained for the other composites and hydrogels.

The scanning electron micrographs of the composites (see Figure 12), demonstrate the anchoring of silver nanoparticles to the surface of the polymeric matrix with a fairly homogeneous distribution, except for composite 18, which exhibited areas covered with NPs intercalated with empty areas.

According to the transmission electron microscopy (TEM) experiments performed on the silver colloid used to prepare the composites, 58% of the nanoparticles had diameters that ranged 1.2–7.4 nm (mean diameter = 3 ± 1 nm), but those <5 nm were not observed in composites by the scanning electron microscopy (SEM) experiments, neither on the outer surface nor in the cross-sections of the materials; note that silver was detected in the EDS analysis of the composites cross-sections [Figure 12(a,b)], but what was detected was most likely residual ionic silver that did not react during the synthesis of the colloid. The absence of nanoparticles with diameters <5 nm in the composites, indicates their possible aggregation when they come in contact with the polymeric matrix, thus increasing in size; it is also probable that nanoparticles <5 nm in size are contained in the composite and do not undergo aggregation, but cannot be detected with the SEM technique under the analysis conditions. If we assume that this last event occurs, it could be stated that the silver detected through the EDS technique in the composite cross-sections not only results from the residual ionic silver but also from the smallest AgNPs (<5 nm in diameter).

CONCLUSIONS

The colloid dispersion of the AgNPs exhibited a wide size distribution, but with a significant population of particles with sizes <10 nm, which corresponds to over 50% of the total NPs present. Therefore, this result is in compliance with the size requirements for exhibiting antibacterial activity.

Because the product of reactivity ratios in both copolymeric systems tends to zero, it can be affirmed that "moderately alternating" copolymerizations occurred. With respect to the VP : AMPS system, there is an "azeotropic point" because both reactivity ratios are lower that the unit, but in relation to the AAm : AMPS system, there is no azeotropic point because only one of its reactivity ratios is slightly higher than the unit.

Comparison of the solid state ^{1}H NMR spectra of the composites to their respective copolymers without nanosilver (hydrogels) reveals an increase in the signal intensity of the amidic protons in the composites with respect to the hydrogels. The most probable explanation is the formation of hydrogen bonds among the carboxyl groups of citrate molecules, which cover the surface of the AgNPs and the "amide pendant groups" of the main chain of the copolymer. When the hydrogen bonds are formed, the amide proton exchange is reduced with deuterated water, which results in a more intense signal in the composite spectrum. Images of composites obtained through the SEM technique show the incorporation of AgNPs on the hydrogel surface. Hydrogel–AgNPs composites with lower MBA percentage retained a higher amount of total silver.

ACKNOWLEDGMENTS

The authors thank FONDECYT (Grant No 1110079), PIA (Grant Anillo ACT-130), and CIPA. H. Valle thanks CONICYT for the scholarship awarded for doctoral studies.

REFERENCES

1. Klasen, H. J. *Burns.* **2000**, *26*, 131.
2. Morones, J. R.; Elechiguerra, J. L.; Camacho, A.; Holt, K.; Kouri, J. B.; Tapia Ramírez, J.; Yacaman, M. J. *Nanotechnology.* **2005**, *16*, 2346.
3. Lok, C. N.; Ho, C. M.; Chen, R.; He, Q. Y.; Yu, W. Y.; Sun, H.; Tam, P. K. H.; Chiu, J. F.; Che, C. M. *J. Proteome Res.* **2006**, *5*, 916.
4. Alt, V.; Bechert, T.; Steinrucke, P.; Wagener, M.; Seidel, P.; Dingeldein, E.; Domann, E.; Schnettler, R. *Biomaterials.* **2004**, *25*, 4383.
5. Min, Y.; Akulut, M.; Kristairsen, K.; Golan, Y.; Israelachvili, J. *Nat. Mater.* **2008**, *7*, 527.
6. Murthy, P. S. K.; Murali Mohan, Y.; Varaprasad, K.; Sreedhar, B.; Mohana Raju, K. *J. Colloid Interface Sci.* **2008**, *318*, 217.
7. Yu, H.; Xu, X.; Chen, X.; Lu, T.; Zhang, P.; Jing, X. *J. Appl. Polym. Sci.* **2007**, *103*, 125.
8. Thomas, V.; Murali Mohan, Y.; Sreedhar, B.; Bajpai, S. K. *J. Appl. Polym. Sci.* **2009**, *111*, 934.
9. Nho, Y. C.; Park, K. R. *J. Appl. Polym. Sci.* **2002**, *85*, 1787.
10. Aguilar, M. R.; Gallardo, A.; Fernández, M. M.; San Román, J. *Macromolecules.* **2002**, *35*, 2036.
11. Ling, J.; Sang, Y.; Huang, C. Z. *J. Pharm. Biomed. Anal.* **2008**, *47*, 860.
12. Martínez, C.; Coello, V. M. *Ciencia UANL.* **2005**, *8*, 346.
13. Malvern Instruments. Zetasizer Nano User Manual MAN0317; Malvern Instruments Ltd.: Malvern, United Kingdom, 2009; Issue 5.0, Chapter 15, pp 1–12.
14. Henglein, A.; Giersig, M. *J. Phys. Chem. B.* **1999**, *103*, 9533.
15. Kunze, J.; Burgess, I.; Nichols, R.; Buess-Herman, C.; Lipkowski, J. *J. Electroanal. Chem.* **2007**, *599*, 147.
16. MacCuspie, R.; Rogers, K.; Patra, M.; Suo, Z.; Allen, A. J.; Martin, M. N.; Hackley, V. A. *J. Environ. Monit.* **2011**, *13*, 1212.
17. Filipe, V.; Hawe, A.; Jiskoot, W. *Pharm. Res.* **2010**, *27*, 796.
18. Mahl, D.; Diendorf, J.; Meyer-Zaika, W.; Epple, M. *Colloids Surf., A.* **2011**, *377*, 386.
19. Yin, H.; Yamamoto, T.; Wada, Y.; Yanagida, S. *Mater. Chem. Phys.* **2004**, *83*, 66.
20. Bune, Y. V.; Barabanova, A. I.; Bogachev, Y. S.; Gromov, V. F. *Eur. Polym. J.* **1997**, *33*, 1313.
21. Rosa, F.; Bordado, J.; Casquilho, M. *J. Appl. Polym. Sci.* **2003**, *87*, 192.
22. Nakajima, T.; Furukawa, H.; Tanaka, Y.; Kurokawa, T.; Osada, Y.; Gong, J. P. *Macromolecules.* **2009**, *42*, 2184.
23. Száraz, I.; Forsling, W. *Polymer.* **2000**, *41*, 4831.

24. García-Fernández, L.; Aguilar, M. R.; Fernández, M. M.; Lozano, R. M.; Giménez, G.; San Román, J. *Biomacromolecules.* **2010**, *11*, 626.
25. Shestakova, P.; Willem, R.; Vassileva, E. *Chem. Eur. J.* **2011**, *17*, 14867.
26. Kurenkov, V. F.; Zhelonkina, T. A. *Russ. J. Appl. Chem.* **2004**, *77*, 307.
27. Travas-Sejdic, J.; Easteal, A. *J. Appl. Polym. Sci.* **2000**, *75*, 619.
28. Rintoul, I.; Wandrey, C. *Polymer.* **2005**, *46*, 4525.
29. Gallardo, A.; Aguilar, M. R.; Abraham, G. A.; San Román, J. *J. Chem. Educ.* **2004**, *81*, 1210.
30. Odian, G. Principles of Polymerization; Wiley: New Jersey, **2004**; p 812.
31. Luo, Y. L.; Xu, F.; Chen, Y. S.; Jia, C. Y. *Polym. Bull.* **2010**, *65*, 181.
32. Dong, H.; Wang, D.; Sun, G.; Hinestroza, J. P. *Chem. Mater.* **2008**, *20*, 6627
33. Pretsch, E.; Bühlmann, P.; Herrera, A.; Martínez, R. Determinación Estructural de Compuestos Orgánicos; Masson: Barcelona, **2002**; p 482.